Available online at www.sciencedirect.com
ScienceDirect
Ceramics International 35 (2009) 2987–2991
CERAMICS INTERNATIONAL
www.elsevier.com/locate/ceramint

Short communication

Inclusion of carbon nanotubes in a hydroxyapatite sol–gel matrix

H. Najafi [a,*], Z.A. Nemati [b], Z. Sadeghian [c]

[a] Institute of Complex Matter Physics (IPMC), Faculty of Basic Science, Swiss Federal Institute of Technology Lausanne (EPFL), 1015 Lausanne, Switzerland
[b] Department of Materials Science and Engineering, Sharif University of Technology, Tehran, Iran
[c] Department of Gas, Research Institute of Petroleum Industry (RIPI), Tehran, Iran

Received 2 February 2009; received in revised form 16 February 2009; accepted 14 March 2009
Available online 15 April 2009

Abstract

In this study, the inclusion of multi-walled carbon nanotubes as the second phase in the hydroxyapatite matrix, in order to improve the mechanical strength, has been performed via the sol–gel process. The stability of carbon nanotube sol with the changes of pH and dispersant values (sodium dodecyl sulfate) was evaluated by zeta potential analysis. The results indicated that synthesis of hydroxyapatite particles in the presence of the carbon nanotubes had the best result in homogenization of the carbon nanotube dispersion and faster crystallization of hydroxyapatite. The crystallization of hydroxyapatite phase was investigated with differential scanning calorimetry (DSC) and X-ray diffraction and the microstructure of the obtained composite powder was studied by electron microscopy.

Keywords: Carbon nanotube; Hydroxyapatite; Crystallization

1. Introduction

Carbon nanotubes (CNTs) have been widely used as reinforcing additive fibers in polymers and metals [1–8] and several recent experiments on the preparation and mechanical characterization of CNT-reinforced ceramic composites have also been reported [9–15]. Some recent studies have even suggested that there may be a bioactive potential for utilization of these composites [16–18]. Therefore, there is an interest for developing CNT–hydroxyapatite composite to combine superior mechanical and biological properties [19].

One of the major and recurring problems encountered in developing CNT-reinforced composites is the tendency of CNTs to aggregate in large bundles and ropes which leads to inhomogeneous dispersion of CNTs in these composite [20]. Obtaining a stable dispersion of CNTs in water indeed is a significant problem and it is also a prerequisite for its application as additives for reinforcement of composite materials [23]. In general there are three principles for dispersing fine particles in water [23]: (I) the repulsion between the particles characterized by with their zeta potential, (II) the steric hindrance of the adsorption layer, and (III) the reduction of hydrophobic linkages among dispersed particles. Sol–gel process has been previously used to disperse CNTs homogeneously in ceramic matrices by entrapping dispersed CNTs in the gel network [21]. Since many applications of CNTs require their dispersion in a variety of organic or aqueous solvents, there have been many investigations on improving CNT solubility [22]. The effective parameters in sol–gel process determine the dispersion and the interfacial bonding states of CNTs in composite.

In this study the inclusion of CNTs in the hydroxyapatite (HA) matrix via the sol–gel process has been investigated and different aspects of the system have been discussed.

2. Experimental procedure

Three methods for the inclusion of 5 wt% multi-walled carbon nanotubes (MWCNTs) in HA via sol–gel process have been studied. In the first method, the HA sol was prepared from nitrate and phosphate solution [24], then CNTs and sodium dodecyl sulfate (SDS), as a dispersant, were added to HA sol by mixing (Fig. 1a). In the second method, HA sol was prepared similar to the first route, and a

* Corresponding author. Tel.: +41 216935414.
E-mail address: Hossein.Najafi@epfl.ch (H. Najafi).

0272-8842/$36.00
doi:10.1016/j.ceramint.2009.03.017

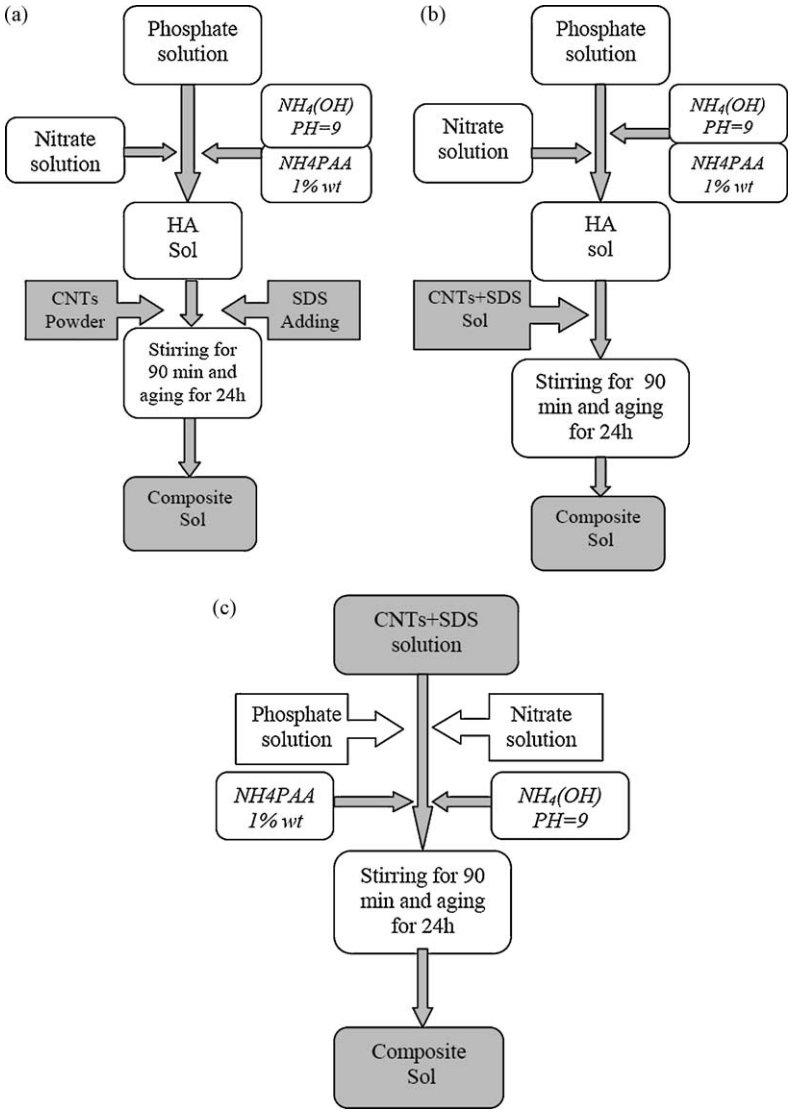

Fig. 1. Different methods of preparation of composite sol: (a) first method, (b) second method, and (c) third method.

sol containing CNTs and SDS which had been prepared before, was added to the HA sol (Fig. 1b). In the third method, HA particles were being produced in the CNT sol which had been prepared in advance (Fig. 1c). The starting materials for sol–gel process were $Ca(NO_3)_2{\cdot}4H_2O$ (Merck, 99% pure), $(NH_4)_2HPO_4$ (Merck, 99% pure), carbon nanotube (Research Center of Petroleum, Iran) and sodium dodecyl sulfate (SDS) as dispersant.

Stability of the CNT sol was evaluated by zeta potential analysis as it has been described previously [23] and was measured as a function of pH and different values of SDS. The gels obtained from the sols were dried at 80 °C and then heat treated at 400 °C for 30 min in order to obtain the HA–CNT composite powder [24]. The formed phases and relative crystallization percentage were characterized with XRD. The thermal behavior was evaluated by differential scanning calorimetry (DSC) analysis. The microstructures of samples were also evaluated by electron microscopy (SEM and TEM).

3. Results and discussion

3.1. Zeta potential analysis

It has been known for a long time that zeta potential is the main factor in sol stability [23]. Based on this fact, the increase in zeta potential would guarantee the sol stability. The analysis of zeta potential is illustrated in Fig. 2 for the CNT sol. As one can see, absolute value of zeta potential has increased with the increase of pH. It seems that a rise in pH value, will result in a higher concentration of $[OH]^-$ which can increase the repulsive forces higher than van der Waals attraction [23]. The change of zeta potential as a function of the *SDS*/*CNT* ratio is also presented in Fig. 2, indicating that the increase in *SDS*/*CNT* ratio up to 4 leads to a rise in the absolute value of zeta potential and after this ratio, there is decline in absolute zeta potential value. It seems that an increase in dispersant concentration up to a certain amount is convenient when reacting with CNT, while *SDS*/*CNT* ratios higher than 4 result in the formation of SDS

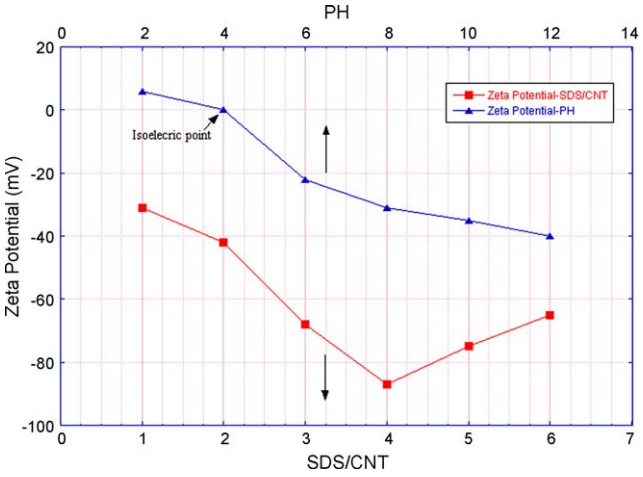

Fig. 2. Zeta potential of CNT sol as a function of pH and dispersant percentage.

agglomerates and the consequent formation of micelles and a logical lowering of sol stability [25].

3.2. DSC analysis

Fig. 3 shows DSC analysis for three sorts of CNT inclusion. As previously known, the HA crystallization temperature is 250 °C which is similar to the previous data [26]. The DSC curves for three different methods have been shown in Fig. 3. In all cases there is an endothermic peak for the moisture removal. But there is also an exothermic peak for HA crystallization.

As shown in Fig. 3a the exothermic peak has appeared at 248 °C for the first method which it is the same as the crystallization temperature of pure HA. But the exothermic peak temperature has decreased to 220 °C and 180 °C for the second and third methods, respectively. The presence of CNT in HA matrix can accelerate crystallization with two possible mechanisms. It is known that the crystallization is highly dependant on diffusion, so the presence of CNTs with high specific surface may be the first reason for the lower crystallization temperature. The presence of CNT can also change the crystallization from homogeneous to heterogeneous

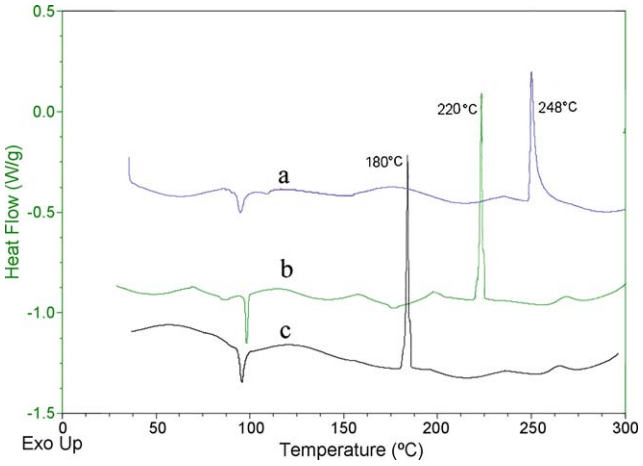

Fig. 3. DSC analysis of samples: (a) first method, (b) second method, and (c) third method.

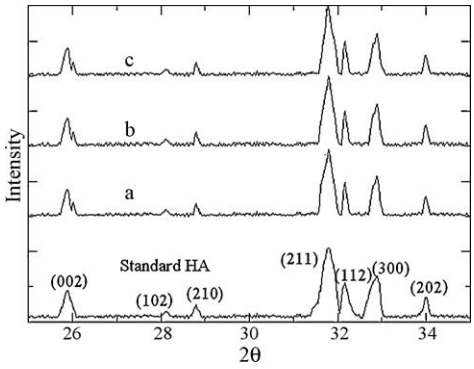

Fig. 4. XRD patterns of samples: (a) first method, (b) second method, and (c) third method.

transformation as the second possible mechanism for reducing the crystallization temperature. Regarding to these two possible mechanisms, presence of carbon nanotubes can enhance the crystallization process. Also better dispersion of CNTs mean higher nucleation sites and diffusion paths and consequently, it can lead to a lower crystallization temperature. Considering the DSC results shown in Fig. 3, it is obvious that in the third method of CNT inclusion, crystallization begins at lower temperature as a result of more harmonized distribution of CNTs in the matrix.

3.3. XRD analysis

XRD patterns of the powders prepared by three different methods have been shown in Fig. 4. The third method has the sharpest peaks among all methods. It is interesting that the peaks at $2\theta = 26^\circ$ in Fig. 4 are diverted to two branches, confirming the presence of CNT. The relative crystallization percentage was measured by a method developed by Pang and Bao [27]. This method compares the intensity of the HA peak at (3 0 0) surface ($I_{3\,0\,0}$) and the intensity of valley between peaks of (3 0 0) and (1 1 2) surfaces ($V_{1\,1\,2/3\,0\,0}$) [27]:

$$X_c = 1 - \left(\frac{V_{112/300}}{I_{300}}\right)$$

The progress of crystallization was monitored and obtained for each method was 74%, 81% and 100%, for the three methods, respectively. It should be noted that the better dispersion of CNTs by third method and resulting higher rate of crystallization, can be considered the reason for the larger crystallized fraction.

3.4. Electron microscopy analysis

SEM images for the powders obtained by three different methods have been shown in Fig. 5. SEM images confirmed the results of DSC and XRD. As shown in Fig. 5, the third method of inclusion (c) has smaller particle size than other methods as well as the second method (b) than first method (a). Fig. 5e shows the TEM images of the resulting powders, which can be concluded from that the average particle size of the synthesized

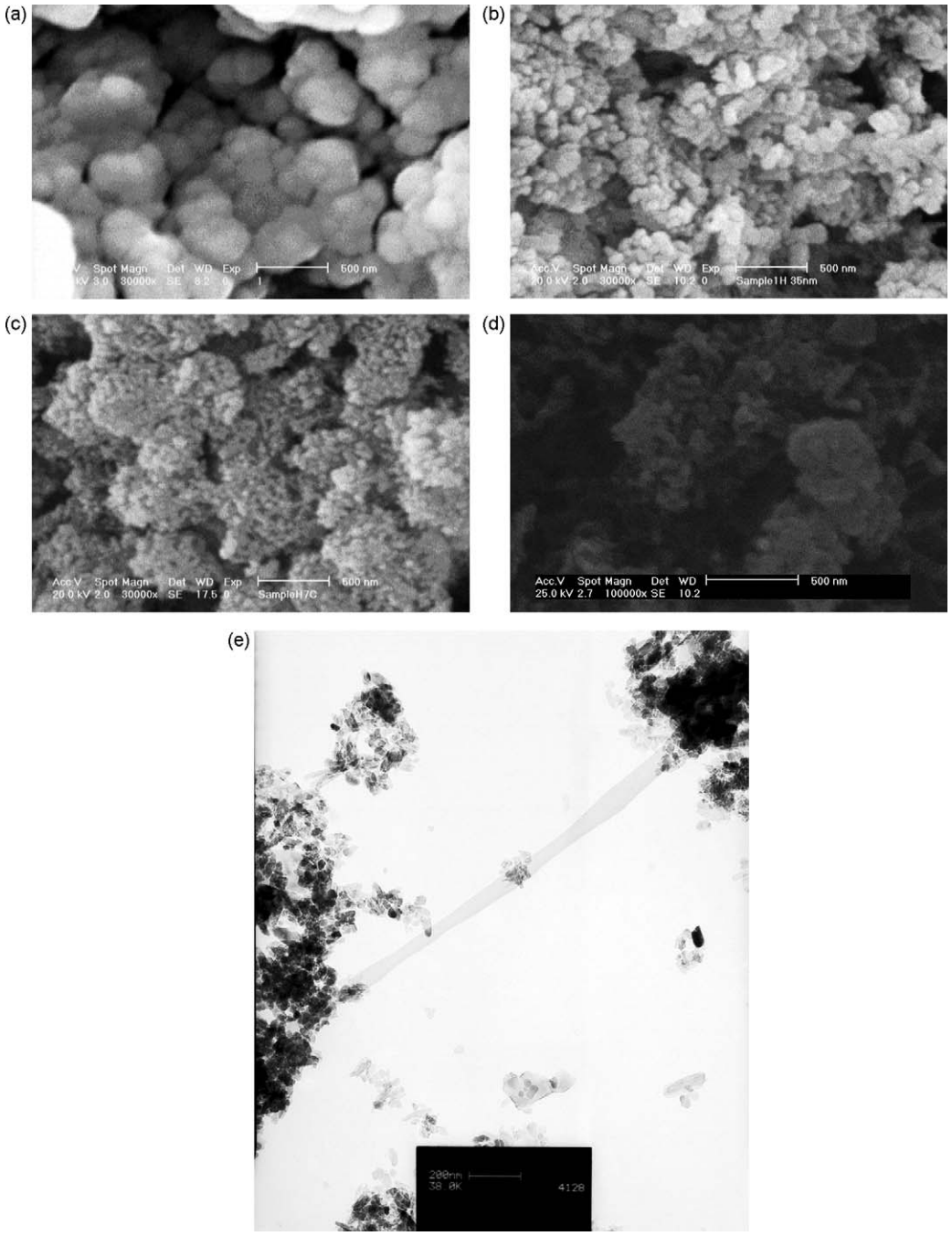

Fig. 5. SEM images for the powders obtained by (a) first method, (b) second method, (c) third method, and (d) third method in higher magnification. (e) TEM image of powder obtained from third method.

HA powders is about 20 nm. It seems, CNT acts as a preferable site for nucleation of HA (Fig. 5d) so if the dispersion of CNTs was more harmonized in matrix then crystallization would begin in a wider scale and particles size would be far smaller than the other two methods. The increased surface area in third method implies higher number of atoms and higher surface defects at the delocalized surfaces fully suitable for human osteoblast cell growth and cell adhesion. Increased surface area is a critical factor for achieving stable scaffold structure for a successful body implant performance.

4. Conclusions

Three methods for the inclusion of 5 wt% MWCNTs in HA were investigated. Results showed that the synthesis of HA particles in the CNT sol which was prepared in advance, leads to an excellent dispersion of CNTs in HA matrix. The presence of CNT in composite of HA–CNT has caused the faster crystallization at lower temperatures compared to pure HA due to heterogeneous nucleation and creation of more diffusion paths.

References

[1] J.C. Grunlun, A.R. Mehrabi, M.V. Bannon, J.L. Bahr, Water-based single-walled-nanotube-filled polymer composite with an exceptionally low percolation threshold, Advanced Materials 16 (2) (2004) 150–153.

[2] R. Sen, B. Zhao, D. Perea, M.E. Itkis, H. Hu, J. Love, et al., Preparation of single-walled carbon nanotube reinforced polystyrene and polyurethane nano-fibers and membranes by electrospinning, Nano Letters 4 (3) (2004) 459–464.

[3] J. Huang, X. Li, J. Xu, H. Li, Well-dispersed single-walled carbon nanotube/polyaniline composite films, Carbon 41 (14) (2003) 2731–2736.

[4] E. Carreno-Morelli, Carbon nanotube–metal matrix composites, in: The Dekker Encyclopedia of Nanoscience and Nanotechnologie, Taylor and Francis, New York, 2006.

[5] E. Carreno-Morelli, et al., Carbon nanotube reinforced metal matrix composites., in: Proceedings of EURO PM 2003, Valence, Spain, October 20–22, 2003.

[6] Kuzumaki, et al., Mechanical characteristics and preparation of carbon nanotubes fiber-reinforced Ti composite, Advanced Engineering Materials 2 (2000) 416–418.

[7] T. Laha, S. Kuchibhatla, S. Seal, W. Li, A. Agarwal, Interfacial phenomena in thermally sprayed multiwalled carbon nanotube reinforced aluminum nanocomposite, Acta Materialia 55 (February (3)) (2007) 1059–1066.

[8] C.F. Deng, D.Z. Wang, X.X. Zhang, Y.X. Ma, Damping characteristics of carbon nanotube reinforced aluminum composite, Materials Letters 61 (June (14–15)) (2007) 3229–3231.

[9] A. Peigney, Ch. Laurent, E. Flahaut, A. Rousset, Carbon nanotubes in novel ceramic matrix nanocomposites, Ceramics International 26 (July (6)) (2000) 677–683.

[10] Balázsi, Z. Kónya, F. Wéber, L.P. Biró, P. Arató, Preparation and characterization of carbon nanotube reinforced silicon nitride composites, Materials Science and Engineering: C 23 (December (6–8)) (2003) 1133–1137.

[11] F. Lupo, R. Kamalakaran, C. Scheu, N. Grobert, M. Rühle, Microstructural investigations on zirconium oxide–carbon nanotube composites synthesized by hydrothermal crystallization, Carbon 42 (10) (2004) 1995–1999.

[12] S. Rul, F. Lefèvre-schlick, E. Capria, Ch. Laurent, A. Peigney, Percolation of single-walled carbon nanotubes in ceramic matrix nanocomposites, Acta Materialia 52 (February (4)) (2004) 1061–1067.

[13] Z. Xia, L. Riester, W.A. Curtin, H. Li, B.W. Sheldon, J. Liang, B. Chang, J.M. Xu, Direct observation of toughening mechanisms in carbon nanotube ceramic matrix composites, Acta Materialia 52 (February (4)) (2004) 931–944.

[14] Y. Wang, Z. Iqbal, S. Mitra, Rapid, low temperature microwave synthesis of novel carbon nanotube–silicon carbide composite, Carbon 44 (13) (2006) 2804–2808.

[15] J. Wang, H. Kou, X. Liu, Y. Pan, J. Guo, Reinforcement of mullite matrix with multi-walled carbon nanotubes, Ceramics International 33 (July (5)) (2007) 719–722.

[16] K.L. Elias, R.L. Price, T.J. Webster, Enhanced functions of osteoblasts on nanometre diameter carbon fibers, Biomaterials 23 (15) (2002) 3279–3287.

[17] M.A. Correa-Duarte, N. Wagner, J. Rojas-Chapana, C. Morsczeck, M. Thie, M. Giersig, Fabrication and biocompatibility of carbon nanotube-based 3D networks as scaffolds for cell seeding and growth, Nano Letters 4 (11) (2004) 2233–2236.

[18] H. Lui, S. Li, J. Zhai, H. Li, Q. Zheng, L. Jiang, et al., Self-assembly of large-scale micropatterns on aligned carbon nanotube films, Angewandte Chemie: International Edition 116 (2004) 1166–1169.

[19] A.W. Ashley, M. Serna, Hydroxyapatite-carbon nanotube composites for biomedical applications: a review, Journal of Applied Ceramic Technology 4 (1) (2007) 1–13.

[20] N. Tagmatarchis, M. Prato, Functionalization of carbon nanotubes by 1,3-dipolar cycloadditions, Journal of Materials Chemistry 14 (4) (2004) 437–439.

[21] C.B. Mo, S.I. Cha, K.T. Kim, K.H. Lee, S.H. Hong, Fabrication of carbon nanotube reinforced alumina matrix nanocomposite by sol–gel process, Materials Science and Engineering A 395 (2005) 124–128.

[22] S.K. Smart, A.I. Cassady, G.Q. Lu, D.J. Martin, The biocompatibility of carbon nanotubes, Carbon 44 (2006) 1034–1047.

[23] J. Linqin, G. Lian, S. Jing, Production of aqueous colloidal dispersions of carbon nanotubes, Journal of Colloid Interface and Science 260 (1) (2003) 89–94.

[24] D.M. Liu, T. Troczynski, W.J. Tseng, Water-based sol–gel synthesis of HA: process development, Biomaterials 22 (13) (2001) 1721–1730.

[25] R.J. Hunter, Foundations of Colloid Science, Oxford University Press, Oxford, 1989.

[26] C.F. Fenga, K.A. Khor, Y.W. Gu, P. Cheang, Analysis of phase changes in plasma-sprayed Ti–6Al–4VrHA composite coatings by DSC, Materials Letters 51 (2001) 88–93.

[27] Y.X. Pang, X. Bao, Influence of temperature, ripening time and calcination on the morphology and crystallinity of HA nanoparticles, Journal of the European Ceramic Society 23 (2003) 1697–1704.